Electrochemistry Communications 185 (2026) 108124

Contents lists available at ScienceDirect

Electrochemistry Communications

journal homepage: www.elsevier.com/locate/elecom

# Hydrogen production via aqueous ammonia electrolysis: electrolyte optimization, product selectivity, and efficiency analysis

Franciele Lamaison Fossaluza, Paulo Firmino Moreira, Claudio Augusto Oller do Nascimento, Maria Anita Mendes *

*Department of Chemical Engineering, Polytechnic School, University of São Paulo, São Paulo, Brazil*

ARTICLE INFO

*Keywords:*
Ammonia electrolysis
Green hydrogen
Faradaic efficiency
Electrochemical energy
GC-TCD

ABSTRACT

This study presents a comprehensive investigation of aqueous ammonia electrolysis as an alternative method for hydrogen production. It explores various experimental conditions, energy, and Faradaic efficiencies, and the underlying electrochemical mechanisms. Cyclic voltammetry and electrolysis tests were conducted at different current densities (ranging from 50 to 700 mA) to determine the optimal conditions for hydrogen gas ($H_2$) generation. Gas chromatography with a thermal conductivity detector (GC-TCD) was used to confirm the production of hydrogen and verify the absence of gaseous nitrogen. Alongside the solution-phase analyses, these findings provide clear evidence for the formation of soluble by-products, primarily nitrite ($NO_2^-$) and nitrate ($NO_3^-$), as both species were detected and quantified in our measurements. The Faradaic efficiency reached 98%, while energy efficiency ranged from 59% to 75%. The results are compared with existing literature, emphasizing ammonia's potential as a sustainable hydrogen carrier and highlighting the current limitations of the process in aqueous media.

## 1. Introduction

Hydrogen is widely acknowledged as a crucial energy vector for the transition to clean, sustainable energy systems [1,2]. It serves as a carbon-free fuel alternative that can be utilized across various sectors, including transportation and chemical industries, facilitating significant decarbonization of energy chains [3]. The growing global interest in the so-called "hydrogen economy" underscores its strategic importance in replacing fossil fuels and integrating renewable energy sources, such as solar and wind, into stable, reliable energy systems [4].

Water electrolysis, while technologically advanced, requires a significant energy input due to its thermodynamic decomposition potential of 1.23 V [5,6]. In contrast, ammonia ($NH_3$) is a promising alternative due to its lower decomposition potential of approximately 0.77 V and its high hydrogen content of 17.6% by weight [2]. Additionally, ammonia is regarded as a convenient hydrogen carrier thanks to its well-established infrastructure for production, storage, and transportation. It also could release hydrogen on demand through catalytic or electrochemical decomposition [7,8].

The electrochemical decomposition of ammonia follows the overall reaction:

$$2NH_3 + 6OH^- \rightarrow N_2 + 3H_2 + 6H_2O$$

Ammonia oxidation at the anode and reduction processes at the cathode are kinetically complex and influenced by factors such as pH, electrode material, and applied potential [5]. Previous studies [1] have highlighted the effectiveness of Pt- and Ni-based catalysts in promoting selective oxidation. However, the overall efficiency still relies on mass transport and internal resistance. **Recent studies have also explored advanced electrocatalytic ammonia oxidation pathways and electrode properties that impact selectivity and efficiency, emphasizing the broader interest in optimizing both catalyst design and reaction conditions for improved hydrogen production and nitrogen-containing product control [9].**

**Electrolyte composition and ionic conductivity play a central role in determining the kinetics, selectivity, and overall efficiency of electrochemical energy conversion processes, particularly in systems involving multi-electron reactions such as ammonia oxidation. The nature of the electrolyte directly influences charge transport, reaction pathways, and interfacial phenomena, thereby impacting hydrogen production efficiency and system stability. Recent studies focusing on ammonia electrolysis systems have demonstrated that electrolyte composition, concentration, and**

* Corresponding author at: Departamento de Engenharia Química- Edifício Semi Industrial, Rua do Lago 250- 05508-080
*E-mail address:* mariaanita.mendes@gmail.com (M.A. Mendes).

https://doi.org/10.1016/j.elecom.2026.108124
Received 12 January 2026; Received in revised form 16 February 2026; Accepted 17 February 2026
Available online 20 February 2026

**ionic transport properties are key parameters governing electrochemical performance and energy efficiency, underscoring the critical importance of electrolyte optimization in ammonia electrolysis processes [10].**

In addition to its favorable thermodynamic properties, ammonia has become increasingly relevant as a practical and scalable hydrogen carrier due to its high volumetric energy density, carbon-free composition, and the well-established global infrastructure for production, storage, and transport [8,11]. In this context, ammonia electrolysis emerges as a key enabling technology; rather than competing with water electrolysis, it provides an efficient pathway to release hydrogen on demand from a stable and energy-dense molecule. Several techno-economic analyses have emphasized that utilizing ammonia as a hydrogen vector can significantly reduce distribution costs, enhance long-distance energy transport, and facilitate the integration of renewable energy sources.

Therefore, understanding and optimizing the electrochemical decomposition of ammonia is essential not only for improving hydrogen generation efficiency but also for advancing ammonia-based energy storage systems within a future low-carbon energy landscape [12–14].

## 2. Materials and methods

### 2.1. Reactor and electrodes

Experiments were conducted in H-type borosilicate reactors (see Fig. 1), using platinum electrodes: a 2.5 $cm^2$ working electrode (WE) and an 11.5 $cm^2$ counter electrode (CE). The counter electrode consisted of coiled platinum wire, and the potentials were measured relative to an Ag/AgCl reference electrode.

### 2.2. Electrolyte and operating conditions

The electrolyte was prepared by dissolving $NH_4Cl$ to achieve a final concentration of 200 mM in a 500 mM $NH_4OH$ aqueous solution. This concentration was determined to be optimal based on a preliminary study that evaluated various electrolyte concentrations. The experiments were conducted at 22 °C and 0.92 atm, with an initial pH of 11. The applied currents ranged from 50 to 100 mA over a 60-min electrolysis period.

### 2.3. Cyclic voltammetry

Cyclic voltammetry (CV) was conducted to assess the redox behavior of ammonia within a potential range from −1.0 V to +0.4 V. The $NH_4Cl$ and $NH_4OH$ system showed the highest cathodic current at around −0.6 V, indicating optimal conditions for hydrogen ($H_2$) evolution.

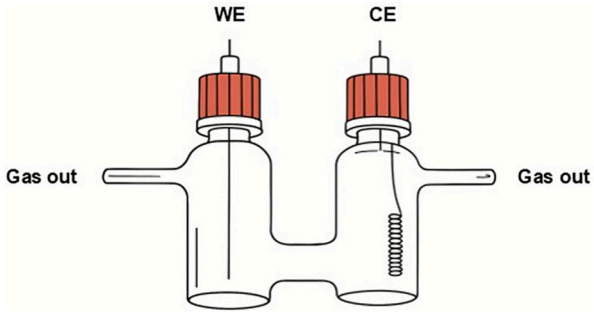


**Fig. 1.** Schematic representation of the H-type borosilicate electrochemical reactor used in the experiments. The system consists of two compartments separated by a glass frit, equipped with platinum working and counter electrodes (2.5 $cm^2$ and 11.5 $cm^2$, respectively) and an Ag/AgCl reference electrode. The configuration allows isolated anodic and cathodic environments, enabling controlled analysis of ammonia oxidation and hydrogen evolution.

### 2.4. Gas and nitrogen species analysis

**Gas quantification was conducted using gas chromatography (GC-TCD) with a Shimadzu 2030 system equipped with a Carboxen 1010 column. Argon was used as the carrier gas, with the injector temperature set to 80 °C and the detector temperature to 100 °C. The concentrations of nitrate and nitrite were determined through colorimetric analysis. Specifically, nitrite and nitrate concentrations in solution were measured using colorimetric test kits from Hanna Instruments: the Nitrite Test Kit HI 3873–0 and the Nitrate Test Kit HI 3874–0, respectively.**

## 3. Results and discussion

### 3.1. Electrolyte concentration effect on CV response

**Cyclic voltammetry (CV) was performed at varying concentrations of ammonium chloride ($NH_4Cl$) from 100 mM to 500 mM. This analysis provided valuable insights into how electrolyte composition affects the electrochemical behavior of the ammonia system. The voltammograms, recorded between − 1.0 and + 0.4 V, displayed significant differences in both anodic and cathodic responses. Notably, in the cathodic region (−0.6 to − 0.8 V), where hydrogen evolution is predominant, the results were particularly striking. Among the tested concentrations (see Fig. 2), the 200 mM $NH_4Cl$ solution showed the highest cathodic current density. It also exhibited a sharp, well-defined peak profile and minimal hysteresis, indicating efficient charge-transfer kinetics, favorable mass transport, and stable interfacial behavior. In contrast, the lowest concentration tested, 100 mM, resulted in significantly reduced currents and less well-defined features. This outcome consists of insufficient ionic strength and increased solution resistance, which hinder electron transfer. At concentrations of 300 mM or higher, the voltammograms became progressively broader and less distinct, showing flattened cathodic waves and increased hysteresis. These distortions can be attributed to mass-transport limitations due to increased viscosity, changes in activity coefficients, and ion-pairing effects at high ionic strength. Additionally, competitive adsorption of $NH_4^+$ or $Cl^-$ species can disrupt the electrochemical double layer and partially inhibit the activity of platinum surface sites. The distinct changes in the waveforms across different concentrations illustrate that both diffusion and interfacial kinetics are strongly influenced by electrolyte composition. Overall, the results confirm that 200 mM $NH_4Cl$ strikes an**

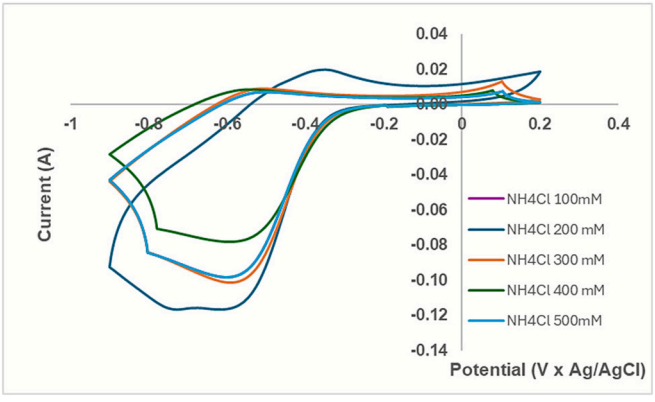


**Fig. 2.** Cyclic voltammograms were recorded for different $NH_4Cl$ concentrations (100–500 mM) in 500 mM $NH_4OH$ at room temperature. The electrolyte with 200 mM $NH_4Cl$ exhibits the highest and most stable cathodic current density in the hydrogen evolution region (−0.6 to −0.8 V), indicating optimal ionic conductivity and superior electrochemical performance relative to the other concentrations tested.

**optimal balance between conductivity, interfacial stability, and charge-transfer efficiency, thereby maximizing hydrogen evolution while avoiding the transport and adsorption limitations observed at higher concentrations. For these reasons, 200 mM $NH_4Cl$ was chosen as the ideal electrolyte concentration for subsequent electrolysis experiments under the studied conditions.**

### 3.2. Voltammetric profiles and electrochemical mechanism

The cyclic voltammogram obtained for the electrolyte containing 200 mM $NH_4Cl$ in 500 mM $NH_4OH$ displays a characteristic profile related to the electro-oxidation of ammonia and hydrogen evolution at the platinum electrode. During the cathodic sweep, a distinct reduction wave emerges between −0.6 and − 0.8 V, corresponding to hydrogen evolution. The current reaches a notable minimum, indicating efficient proton reduction facilitated by the buffer capacity of the $NH_4^+/NH_3$ system and the favorable ionic conductivity at this concentration. The smooth, continuous increase in current magnitude throughout the cathodic branch suggests that mass transport does not limit the process and that the electrode surface remains active during the scan. During the anodic sweep, the voltammogram exhibits a clear oxidation transition beginning near −0.3 V and extending toward positive potentials, marked by an anodic shoulder that signifies the onset of ammonia oxidation. The anodic current remains relatively modest, which is expected for platinum in alkaline ammonium media. The absence of significant peak splitting or hysteresis indicates a stable electrode-solution interface with minimal accumulation of adsorbed intermediates, such as $*NH_x$ species. The nearly symmetrical loop and the relatively small separation between the forward and reverse scans confirm that the system demonstrates quasi-reversible behavior, with charge-transfer kinetics not significantly hindered by surface poisoning at this electrolyte concentration. Overall, the distinct voltammogram shape, characterized by a pronounced cathodic wave and a smooth anodic response, supports the conclusion that 200 mM $NH_4Cl$ provides an optimal balance of conductivity, buffer capacity, and interfacial stability, enabling effective hydrogen evolution and controlled ammonia oxidation during the potential cycle. [15].

### 3.3. Selection of applied currents for electrolysis experiments

**The current values of 50, 75, and 100 mA used in the electrolysis experiments were determined based on the voltammetric behavior of a 200 mM $NH_4Cl$ electrolyte. The cyclic voltammetry (CV) results showed a well-defined hydrogen evolution region between − 0.6 and − 0.8 V, where the system exhibited stable charge-transfer kinetics and no signs of mass-transport limitations. This cathodic window corresponds to a potential range where the current increases sharply and consistently, indicating that hydrogen evolution can occur efficiently under controlled current conditions. The 100 mA current was selected to explore conditions near the upper boundary of the system's stable electrochemical response, providing insights into hydrogen generation at higher reaction rates without exceeding the onset of polarization effects indicated by the CV profile. The intermediate current of 75 mA represents a balanced regime in which the electrode operates efficiently within the hydrogen evolution interval, enabling assessment of energy efficiency and Faradaic performance under moderate kinetic demands. Lastly, a current of 50 mA was chosen as a conservative operating condition, minimizing overpotential and avoiding the risk of diffusion-driven deviations, thereby enabling a precise evaluation of baseline system efficiency.**

Together, these three current levels establish a systematic framework for analyzing the influence of electron flux on hydrogen production, ammonia oxidation pathways, and energy consumption, while remaining entirely consistent with the electrochemical behavior observed in the voltammetric characterization.

### 3.4. Gas chromatography analysis

**To achieve precise detection and quantification of gases produced during ammonia electrolysis, a series of optimization experiments was conducted using gas chromatography with a thermal conductivity detector (GC-TCD). The experiments focused on adjusting key operational parameters, including selecting the carrier gas and working temperatures within the system.**

Initial tests revealed that helium, commonly used as a carrier gas, was not suitable for hydrogen detection because its thermal conductivity was too similar to hydrogen's. Consequently, argon was chosen as the preferred carrier gas, providing better contrast and sensitivity for detecting hydrogen peaks. Further adjustments were made to the detector and injector temperatures, as well as to the flow rates, to enhance resolution and signal intensity.

After systematic testing, the optimal working conditions were established as follows: injector temperature at 80 °C, column temperature at 60 °C, detector temperature at 100 °C, and detector current at 30 mA. Both the carrier gas and make-up gas were set to argon with a flow rate of 3.0 mL/min. The injection method employed was split mode with an 80:20 ratio. Under these conditions, the retention times were clearly defined: hydrogen at 2.11 min, oxygen at 3.45 min, and nitrogen at 3.57 min (Fig. 3). These optimized parameters allowed for reliable separation and quantification of the target gases, facilitating consistent monitoring of hydrogen production during electrolysis experiments.

The chromatogram obtained from the ammonia electrolysis experiment, conducted at 200 mA for 60 min, displayed three distinct peaks corresponding to hydrogen ($H_2$), oxygen ($O_2$), and nitrogen ($N_2$). The hydrogen peak at approximately 2.11 min was clearly associated with the electrochemical reduction of ammonia at the cathode, confirming successful hydrogen generation under the specified conditions.

However, the peaks observed at 3.45 min ($O_2$) and 3.57 min ($N_2$) do not correspond to products formed during the electrolysis reaction. Instead, these signals are attributed to residual atmospheric gases, specifically air, that entered the system due to incomplete sealing of the electrolysis reactor. This interpretation is supported by the close correlation between the intensities and retention times of the $O_2$ and $N_2$ peaks and those of atmospheric air standards, and by their consistent presence in control samples. Therefore, these peaks should not be interpreted as evidence of ammonia oxidation to nitrogen gas or water electrolysis producing oxygen; instead, they indicate background contamination. **The GC-TCD calibration was performed using direct injections of pure $N_2$ without dilution. The lowest reliably detected injection volume was 20 μL, corresponding to approximately 0.82 μmol of $N_2$ under ambient conditions (1 atm, 25 °C). Therefore, any electrochemically generated $N_2$ below this amount may remain undetected. Therefore, trace amounts of electrochemically generated $N_2$ or $O_2$ below this threshold cannot be completely excluded, although no current-dependent increase was observed.**

**Due to the setup not being entirely airtight, ambient oxygen and nitrogen diffused into the gas collection line and were subsequently detected during chromatographic analysis. Future experiments will require improved sealing of the system to ensure accurate quantification of reaction products. Moreover, no detectable nitrogen gas ($N_2$) was observed, suggesting that ammonia oxidation did not completely convert to nitrogen gas; instead, it likely formed nitrate ($NO_2^-$) and nitrite ($NO_3^-$) species in solution. The observed product distribution is governed by the combined effect of the Pt electrode and the alkaline $NH_4Cl/NH_4OH$ electrolyte. Platinum is known to promote ammonia oxidation through adsorbed $NH_x*$ intermediates, but under the applied potentials and alkaline conditions used in this study, complete oxidation to $N_2$ is kinetically unfavorable. Instead, parallel oxidation pathways leading to soluble $NO_x$ species become dominant. Additionally, the presence of chloride ions and high hydroxide concentration influences surface coverage and reaction kinetics,**

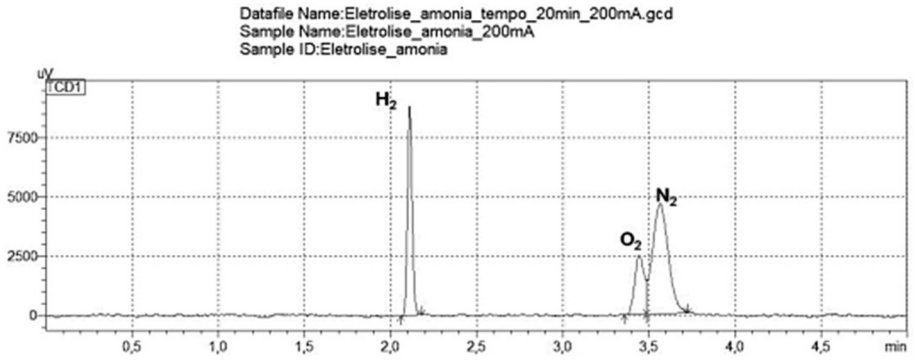


**Fig. 3.** Gas chromatography (GC-TCD) chromatograms for samples collected during ammonia electrolysis. The profiles show a distinct hydrogen peak and confirm the absence of nitrogen gas formation under all applied current conditions, indicating incomplete oxidation of ammonia to $N_2$ in the present system.

**favoring nitrate formation over $N_2$ evolution Similar results reported by Christensen et al. (2020) indicate that complete oxidation to $N_2$ is strongly dependent on the anode material and the applied potential. Catalysts such as Pt—Ru or Ni—Co are known to enhance the selectivity of ammonia oxidation.**

### 3.5. Analysis of nitrite, nitrate, and hydrogen production

**Nitrite and nitrate concentrations were measured using colorimetric test kits from Hanna Instruments: the Nitrite Test Kit HI 3873–0 and the Nitrate Test Kit HI 3874–0.** Table 1 **summarizes the concentrations of the aqueous nitrogen species and the corresponding hydrogen volumes measured for each applied current.**

**Across all experiments, nitrate ($NO_3^-$) was the dominant soluble oxidation product, while nitrite ($NO_2^-$) was present only in small quantities. At a current of 100 mA, where hydrogen production was highest (0.73 mL/min), the nitrate concentration was also relatively high (40 mg/L). This suggests that higher currents favor partial ammonia oxidation but do not necessarily lead to higher nitrite conversion. In contrast, the experiments at 75 mA and 50 mA exhibited similar nitrate concentrations (60 mg/L each), despite differing hydrogen outputs (0.58 mL/min and 0.35 mL/min, respectively). This indicates that nitrate formation may not depend linearly on current; rather, it is likely influenced by complex kinetic factors, such as local pH gradients, mass transport, and surface reaction mechanisms at the anode. Nitrite levels remained low across all conditions (0.1–0.2 mg/L), which aligns with existing literature indicating that $NO_2^-$ is typically an unstable intermediate that rapidly oxidizes to $NO_3^-$ in alkaline environments.**

**A qualitative comparison indicates that higher hydrogen production, such as 0.73 mL/min at 100 mA, does not necessarily lead to an increased formation of nitrogen-containing by-products. While it is expected that hydrogen output rises with the applied current, the accumulation of nitrate seems to follow a more complex pathway. This implies that the oxidation of ammonia does not completely balance hydrogen production in terms of nitrogen mass closure.**

**Despite the formation of $NO_2^-$ and $NO_3^-$ in solution, the total nitrogen measured in the aqueous species is considerably lower than the stoichiometric amount anticipated from ammonia decomposition. Notably, no gaseous nitrogen ($N_2$) was detected using gas chromatography with thermal conductivity detection (GC-TCD), indicating that the missing nitrogen is not in a gaseous form.**

The unexplained nitrogen may exist in other dissolved NOx species not accounted for in this study, such as $NO_2$, $NO_3$, and $NH_2OH$, or in intermediate adsorbed species on the electrode surface, like NHx*, N*, and NOx*. This phenomenon has been documented in catalytic ammonia oxidation mechanisms, particularly in the formation of surface passivation layers on nickel-based electrodes. Consequently, the incomplete recovery of nitrogen indicates the presence of additional oxidation pathways and surface-bound intermediates that need further investigation [16,17].

**The time-resolved hydrogen production profiles illustrated in** Fig. 4 **clearly demonstrate how applied current influences the kinetics of hydrogen evolution during aqueous ammonia electrolysis. All three curves show approximately linear increases over the 60-**min **experiment, indicating that the system operated under stable electrochemical conditions, without noticeable mass-transport limitations or electrode passivation within the tested range.**

At a current of 50 mA, the hydrogen generation rate is the lowest, reaching around 21 mL by the end of the experiment. The gentle slope of this curve reflects the lower electron flux available for the cathodic

**Table 1**
Nitrite, nitrate, and hydrogen production during aqueous ammonia electrolysis at different applied currents. The results reflect the distribution of nitrogen-containing products and the corresponding hydrogen generation rates under steady-state operation.

| Applied Current | Nitrite ($NO_2^-$) mg/L | Nitrate ($NO_3^-$) mg/L | $H_2$ Produced (mL/h) |
|---|---|---|---|
| 100 mA | **0.2 mg/L** | 40 mg/L | **43 mL/h** |
| 75 mA | **0.1 mg/L** | 60 mg/L | **34 mL/h** |
| 50 mA | **0.1 mg/L** | 60 mg/L | **21 mL/h** |

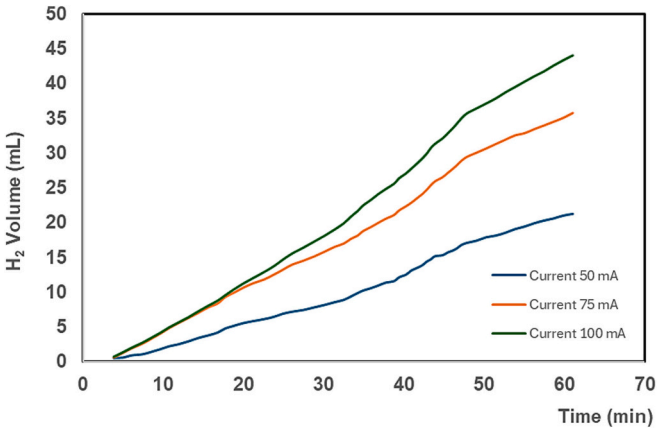


**Fig. 4.** Hydrogen production as a function of time during ammonia electrolysis at applied currents of 50, 75, and 100 mA. Higher applied currents result in increased hydrogen evolution rates, with 100 mA producing approximately 0.98 mL/min, 75 mA yielding 0.58 mL/min, and 50 mA generating 0.35 mL/min. The results demonstrate the direct proportionality between applied current and hydrogen generation efficiency.

hydrogen evolution reaction. When the current is increased to 75 mA, the slope becomes steeper, and the final volume of hydrogen produced reaches approximately 35 mL. This suggests a nearly proportional increase in hydrogen production, as predicted by Faraday's law, while maintaining a linear, stable profile throughout the experiment.

**The results at 100 mA support this trend, yielding the highest hydrogen volume of approximately 0.73 mL/min and the steepest curve among the three tested currents. The preserved linearity, even at the highest current, indicates that neither ammonia depletion nor significant diffusion limitations occurred, and that the electrode remained active throughout the entire electrolysis period.**

**A detailed comparison of the curves reveals that the increase in hydrogen production is not perfectly proportional to the increase in applied current. For instance, when the current is doubled from 50 to 100 mA, the hydrogen volume increases by roughly 110%, in contrast, increasing the current from 75 to 100 mA results in only a 25% increase, despite representing a 33% increase. This slight deviation from ideal proportionality suggests the presence of factors such as ohmic losses, additional side reactions, or competing ammonia oxidation pathways. These pathways, including nitrate and nitrite formation, become more significant at higher currents, potentially consuming ammonia or intermediates that would otherwise contribute to hydrogen production.**

**Overall, the linearity of all curves indicates that ammonia concentration, electrolyte conductivity, and electrode surface activity remained adequate for sustained hydrogen evolution throughout the experiment. These trends suggest that current intensity strongly influences the reaction kinetics of hydrogen production. However, the imperfect proportionality between current and hydrogen volume is consistent with the incomplete nitrogen balance observed in the system. It is important to note that a full quantitative nitrogen mass balance was not attempted in this study. Only gaseous products ($H_2$ and $N_2$) and aqueous nitrite and nitrate species were experimentally quantified. Other possible nitrogen-containing intermediates, such as hydroxylamine ($NH_2OH$), dissolved $NO_x$ species, or surface-adsorbed intermediates ($NH_x$*, N*, $NO_x$*), were not directly measured. As a result, the nitrogen balance discussed here is partial and qualitative rather than fully quantitative. This limitation supports the interpretation that parallel oxidation pathways and the formation of adsorbed intermediates play a significant role in ammonia electrolysis under the conditions studied.**

### 3.6. Faradaic and energy efficiencies

**To assess the performance of aqueous ammonia electrolysis under various operating conditions, experiments were conducted at current intensities of 50 mA, 75 mA, and 100 mA. These specific current levels were chosen to ensure that the experimental conditions were comparable to those used in preliminary tests, where optimal performance was observed at 200 mA. The selected values aim to assess both energy and Faradaic efficiencies under controlled, reproducible conditions, enabling consistent comparison with previous optimization experiments. Faradaic efficiency was calculated based on the experimentally measured hydrogen volume relative to the theoretical hydrogen yield derived from the total charge passed. Throughout all tests, the Faradaic efficiency remained high, with corrected values of approximately 96.4%, 98.2%, and 92.9%, respectively. These results indicate that a significant portion of the electrical charge was effectively converted into hydrogen gas, particularly at 75 mA, which yielded the highest Faradaic efficiency. Two scenarios were considered when evaluating energy efficiency: one based on the actual potential across the electrochemical cell and the other on the total potential supplied by the power source. The latter includes system losses, such as internal resistance and overpotential. When calculated using the cell potential, energy efficiency ranged from 66.7% to 75.0%, demonstrating that the electrochemical reaction itself was relatively efficient. However, when accounting for the full system losses, energy efficiency dropped to 33%–36%, indicating significant energy dissipation outside the reaction zone, likely due to overpotential and thermal losses [1,4]. These findings highlight the importance of optimizing cell design and operating parameters to reduce resistive losses and enhance overall system performance. Among the tested conditions, a current of 75 mA achieved the best balance between hydrogen production and energy efficiency. In contrast, while 100 mA produced higher hydrogen output, it also increased energy consumption. The results from the experiments align with reported efficiencies for ammonia electrolysis systems that utilize platinum (Pt) and nickel (Ni) catalysts, which range from 60% to 80% [5,18]. The calculated energy efficiency, based on the Gibbs free energy (237 kJ/mol for $H_2$), was 62.5%. This aligns well with values reported for reference catalytic systems [4]. The current results (Tables 2 and 3) closely align with those of** Mazloomi and Gomes [4]**, who reported Faradaic efficiencies ranging from 90% to 95% in optimized ammonia electrolysis systems. In this case, the overall yield relative to the ammonia consumed was 1.2%. This can be attributed to incomplete reagent conversion in aqueous media and to adsorption of intermediates on electrode surfaces [18].**

### 3.7. Comparison with literature data

The current results (Table 3) closely align with those of Mazloomi and Gomes [4], who reported Faradaic efficiencies of 90%–95% in optimized ammonia electrolysis systems. The overall yield relative to the consumed ammonia was 1.2%, attributed to incomplete conversion of reactants in aqueous medium and the intermediate adsorption on electrode surfaces [18]. **From a techno-economic perspective, the results summarized in Table 3 indicate that ammonia electrolysis in an $NH_4Cl/NH_4OH$ electrolyte can achieve Faradaic and energy efficiencies comparable to those reported for conventional alkaline ammonia electrolysis and even water electrolysis systems. Unlike water electrolysis, ammonia electrolysis benefits from a lower theoretical decomposition voltage and avoids the need for ultrapure water, which can reduce both energy demand and operational costs. Moreover, the use of aqueous ammonia as a hydrogen carrier leverages existing large-scale infrastructure for ammonia production, storage, and transportation, potentially lowering capital and distribution costs. Although additional energy losses related to cell resistance remain a challenge, the present system demonstrates that efficient hydrogen generation from ammonia can be achieved under mild conditions, supporting its practical relevance for decentralized hydrogen production and on-demand hydrogen release.**

## 4. Conclusions

The results of this study demonstrate that electrolysis of aqueous

**Table 2**
Electrical energy consumption and associated efficiencies for ammonia electrolysis at 50, 75, and 100 mA. Values are reported for both cell potential and power source, allowing direct comparison of system-level and device-level performance.

| Current (mA) | Electrical Energy (Cell) | Efficiency (Cell) | Electrical Energy (Power Source) | Efficiency (Power Source) |
|---|---|---|---|---|
| 50 | **6.0 J** | **66.7%** | **12.0 J** | **33.3%** |
| 75 | **9.9 J** | **67.7%** | **20.3 J** | **33.0%** |
| 100 | **14.4 J** | **75.0%** | **30.0 J** | **36.0%** |

**Table 3**
Comparison of Faradaic and energy efficiencies obtained in this work **(calculated based on the cell voltage)** with reported values from the literature for different ammonia electrolysis systems and electrolyte compositions.

| Study | Catalyst / Electrode | Electrolyte Composition | Operating Conditions* | Main Products | Faradaic Efficiency (%) | Energy Efficiency (%) |
|---|---|---|---|---|---|---|
| This work | Pt foil | $NH_4Cl$ 200 mM + $NH_4OH$ 500 mM | RT, 0,98 atm, aqueous | $H_2$ (gas), $NO_3^-$ (aq), trace $NO_2^-$ | 96–98 | 59–75 |
| Christensen et al. [1] | Pt-based electrode | 1 M KOH + $NH_3$ (g) | RT, 1 atm | $H_2$, $N_2$ | 94 | 68 |
| Lan et al. [2] | Pt electrode | 1 M NaOH + $NH_3$ (aq) | RT, 1 atm | $H_2$, $N_2$ | 95 | 60–70 |
| Mazloomi and Gomes [4] | Ni-based catalyst | 0.5 M NaOH + $NH_3$ (aq) | RT, 1 atm | $H_2$, $N_2$ | 90–95 | 65 |
| Zhao et al. [19] | Pt/Ni catalyst | Alkaline medium | RT, 1 atm | $H_2$, $N_2$ | 97 | 72 |
| Gupta et al. [7] | Transition metal catalyst | 1 M KOH + $NH_3$ | RT, 1 atm | $H_2$, $N_2$ / NOx | 93 | 70 |

ammonia is an effective method for recovering hydrogen. This reinforces ammonia's potential as one of the most promising hydrogen carriers in a low-carbon energy system. With a hydrogen content of 17.6 wt% and a low thermodynamic decomposition potential, ammonia can be synthesized, transported, and stored using existing industrial infrastructure, providing a practical and safe way to store renewable energy.

Our findings show that this stored hydrogen can be released on demand through electrochemical decomposition under mild conditions. The $NH_4Cl/NH_4OH$ electrolyte system achieved high Faradaic efficiencies (92–98%), indicating that nearly all the electrical charge was converted into molecular hydrogen. Hydrogen production increased proportionally with the applied current, reaching 0.73 mL/min at 100 mA, while energy efficiencies ranged from 59% to 75%, aligning with literature reference systems.

**Gas chromatography confirmed that hydrogen was the only gaseous product, demonstrating that ammonia was selectively converted to hydrogen without detectable nitrogen gas ($N_2$) under the tested conditions. Although the oxidation of ammonia did not fully proceed to $N_2$, primarily resulting in nitrate and minor nitrite formation, this limitation does not impact the main objective of the process: efficient hydrogen regeneration from ammonia. The incomplete nitrogen balance suggests the presence of unquantified dissolved $NO_x$ species and surface-adsorbed intermediates, which should be investigated in future mechanistic and materials-focused studies.**

Overall, these results highlight that ammonia is an excellent hydrogen carrier and that ammonia electrolysis offers a viable pathway to regenerate hydrogen under mild, controllable, and electrically driven conditions. This combination of practicality, high efficiency, and compatibility with existing infrastructure emphasizes the strategic value of ammonia electrolysis for distributed hydrogen production within emerging low-carbon energy systems.

## AI Statement

The authors utilized AI-assisted tools, including ChatGPT, OpenAI, Scispace, and Grammarly, to aid language editing, text revision, refining figure captions, and enhancing clarity and organization. All scientific content, data interpretation, analysis, conclusions, and decisions regarding the structure and accuracy of the manuscript were solely generated, verified, and validated by the authors. The AI tools were used under human oversight and did not contribute to the originality or authorship of the work.

## CRediT authorship contribution statement

**Franciele Lamaison Fossaluza:** Writing – review & editing, Methodology, Investigation, Formal analysis, Conceptualization. **Paulo Firmino Moreira:** Software, Methodology, Formal analysis. **Claudio Augusto Oller do Nascimento:** Funding acquisition. **Maria Anita Mendes:** Writing – review & editing, Writing – original draft, Methodology, Formal analysis, Data curation, Conceptualization.

## Declaration of competing interest

The authors declare that they have no known competing financial interests or personal relationships that could have appeared to influence the work reported in this paper.

## Acknowledgements

The authors acknowledge financial support from the São Paulo Research Foundation (FAPESP), grant #2013/50218-2. Petronas, grant # 403902, for their financial support. The authors also acknowledge the Brazilian National Oil, Natural Gas, and Biofuels Agency (ANP) for the strategic relevance of its support through the R&D levy regulation.

## Data availability

Data will be made available on request.

## References

[1] Claus Hviid Christensen, Rasmus Zink Sørensen, Tue Johannessen, Ulrich J. Quaade, Karoliina Honkala, Tobias D. Elmøe, Rikke Køhler, Jens K. Nørskov, Metal ammine complexes for hydrogen storage, J. Mater. Chem. 15 (38) (2005) 4106–4108, https://doi.org/10.1039/B511589B.
[2] R. Lan, John T.S. Irvine, Shanwen Tao, Ammonia and related chemicals as potential indirect hydrogen storage materials, Int. J. Hydrog. Energy 37 (2) (2012) 1482–1494, https://doi.org/10.1016/j.ijhydene.2011.10.004.
[3] Muhammad Shujaat Mubarik, Angappa Gunasekaran, Sharfuddin Ahmed Khan, Muhammad Faraz Mubarak, Decarbonization through supply chain innovation: role of supply chain collaboration and mapping, J. Clean. Prod. 507 (September 2024) (2025) 145492, https://doi.org/10.1016/j.jclepro.2025.145492.
[4] K. Mazloomi, Chandima Gomes, Hydrogen as an energy carrier: prospects and challenges, Renew. Sust. Energ. Rev. 16 (5) (2012) 3024–3033, https://doi.org/10.1016/j.rser.2012.02.028.
[5] J. Allen, Bard, R. Larry, Faulkner, Electrochemical Methods: Fundamentals and Applications. Edited by Wiley, Second, Willey, 2011.
[6] J.D. Holladay, J. Hu, D.L. King, Y. Wang, An overview of hydrogen production technologies, Catal. Today 139 (4) (2009) 244–260, https://doi.org/10.1016/j.cattod.2008.08.039.
[7] T. Gupta, S.S. Sanyam, Anirban Mondal, Biswajit Mondal, Electrochemical Ammonia oxidation with a homogeneous molecular redox mediator, Chem. Sci. 16 (31) (2025) 14377–14383, https://doi.org/10.1039/d5sc00730e.
[8] A. Valera-Medina, H. Xiao, M. Owen-Jones, W.I.F. David, P.J. Bowen, Ammonia for power, Prog. Energy Combust. Sci. 69 (2018) 63–102, https://doi.org/10.1016/j.pecs.2018.07.001.
[9] H. Liu, C.J. Yang, C.L. Dong, J. Wang, X. Zhang, A. Lyalin, T. Taketsugu, Z. Chen, D. Guan, X. Xu, Z. Shao, Z. Huang, Electrocatalytic Ammonia oxidation to nitrite and nitrate with NiOOH-Ni, Energy Mater. 14 (2401675) (2024), https://doi.org/10.1002/aenm.202401675.
[10] H. Liu, X. Xu, D. Guan, Z. Shao, Minireview on the electrocatalytic Ammonia oxidation reaction for hydrogen production and sewage treatment, Energy Fuel 38 (2) (2023), https://doi.org/10.1021/acs.energyfuels.3c04452.
[11] D.R. MacFarlane, Pavel V. Cherepanov, J. C, Bryan H.R. Suryanto, R.Y. Hodgetts, Jacinta M. Bakker, Federico M. Ferrero Vallana, Alexandr N. Simonov, A roadmap to the Ammonia economy, Joule 4 (6) (2020) 1186–1205, https://doi.org/10.1016/j.joule.2020.04.004.
[12] J.S. Cardoso, R.C. Valter Silva, M.J. Rocha, M.C. Hall, Daniela Eusébio, Ammonia as an energy vector: current and future prospects for low-carbon fuel applications

in internal combustion engines, J. Clean. Prod. 296 (2021), https://doi.org/10.1016/j.jclepro.2021.126562.
[13] R. Estevez, J.L. Francisco, A.A. Romero, Diego Luna, Laura Aguado-deblas, Felipa M. Bautista, Urrent research on green Ammonia ($NH_3$) as a potential vector energy for power storage and engine fuels: a review, Energies 16 (1) (2023), https://doi.org/10.3390/en161454514.
[14] S. Giddey, S.P.S. Badwal, C. Munnings, M. Dolan, Ammonia as a renewable energy transportation media, ACS Sustain. Chem. Eng. 5 (11) (2017) 10231–10239, https://doi.org/10.1021/acssuschemeng.7b02219.
[15] E. Atala, G. Velásquez, C. Vergara, C. Mardones, J. Reyes, R.A. Tapia, F. Quina, et al., Mechanism of pyrogallol red oxidation induced by free radicals and reactive oxidant species. A kinetic and Spectroelectrochemistry study, J. Phys. Chem. B 117 (17) (2013), https://doi.org/10.1021/jp400423w.
[16] T.E. Bell, L. Torrente-Murciano, H2 production via Ammonia decomposition using non-Noble metal catalysts: a review, Top. Catal. 59 (15–16) (2016) 1438–1457, https://doi.org/10.1007/s11244-016-0653-4.
[17] H.Y. Liu, Hannah M.C. Lant, C.C. Cody, Jana Jelušić, Robert H. Crabtree, Gary W. Brudvig, Electrochemical Ammonia oxidation with molecular catalysts, ACS Catal. 13 (7) (2023) 4675–4682, https://doi.org/10.1021/acscatal.3c00032.
[18] I. Staffell, A.V.A. Daniel Scamman, P.E. Paul Balcombe, Paul Ekins Dodds, Nilay Shah, Kate R. Ward, The role of hydrogen and fuel cells in the global energy system, Energy Environ. Sci. 12 (2) (2019) 463–491, https://doi.org/10.1039/c8ee01157e.
[19] Y. Zhao, J.Z. Li Wang, Weimin Gong, Hongchen Guo, Decomposition of Ammonia by atmospheric pressure AC discharge: catalytic effect of the electrodes, Catal. Today 211 (2013) 72–77, https://doi.org/10.1016/j.cattod.2013.03.027.